Identification of a thioredoxin reductase from *Babesia microti* during mammalian infection

Shaoruo Zhao[1] · Haiyan Gong[1] · Yongzhi Zhou[1] · Houshuang Zhang[1] · Jie Cao[1] ·
Jinlin Zhou[1,2]

Abstract *Babesia microti* is the primary causative agent of
human babesiosis worldwide and associated with increased
human health risks and the safety of blood supply. The para-
site replicates in the host's red blood cells, thus, in order to
counteract the oxidative stress and toxic effects, parasites em-
ploy a thioredoxin (Trx) system to maintain a redox balance.
Since thioredoxin reductase (TrxR) plays a critical role in the
system, in this study, we report the cloning, expression, and
functional characterization of a novel TrxR from *B. microti*
(BmiTrxR). The complete gene BmiTrxR was obtained by
amplifying the 5′ and 3′ regions of messenger RNA
(mRNA) by RACE. The full-length complementary DNA
(cDNA) of BmiTrxR was 1766 bp and contained an intact
open reading frame with 1662 bp that encoded a polypeptide
with 553 amino acids. Molecular weight of the predicted pro-
tein was 58.4 kDa with an isoelectric point of 6.95, similar to
high molecular weight TrxR. The recombinant protein of
BmiTrxR was expressed in a His-fused soluble form in
Escherichia coli. The native protein BmiTrxR was identified
with the mouse anti-BmiTrxR polyclonal serum by western
blotting and IFAT. Moreover, the enzyme showed a disulfide
reductase activity using DTNB as substrate and catalyzed the
NADPH-dependent reduction of Trx. Auranofin, a known in-
hibitor of TrxR, completely abrogated the activity of the

recombinant enzyme in vitro. These results not only contrib-
ute to the understanding of redox pathway in this parasite but
also suggest that BmiTrxR could be a potential target for the
development of novel strategies to control *B. microti* thus
reducing the incidence of babesiosis.

Keywords *Babesia microti* · Thioredoxin reductase · Enzyme
activity · Auranofin · Drug target

Introduction

Babesiosis, caused by *Babesia*, is an emerging tick-borne dis-
ease in humans. The parasite replicates in the host's red blood
cells, leading to myalgia, anemia, fatigue, and fever hematu-
ria. Most severe infections are predominant in the elderly and
in splenectomized or immunocompromised hosts (Holmgren
and Lu 2010; Homer et al. 2000). *Babesia microti*, one of the
severe pathogenic agents, undergoes a complex life cycle by
infecting both arthropod ticks and mammalian hosts (rodents
and human). In addition, the disease can be transmitted by
blood transfusion and congenital transmission, which poses
a risk to the blood supply. As blood transfusions are neces-
sary for some illnesses, preventing the occurrence of babe-
siosis is based primarily on increasing the awareness of the
public to the potential risks. Despite the diagnostic and pre-
ventive advances, the efficacy of currently used drugs to
treat babesiosis is reported to vary in different strains of this
parasite species. Therefore, new targets are needed to curb
the emergence of drug-resistant *Babesia* parasites
(Schnittger et al. 2012; Song et al. 2012).

In mammalian hosts, *Babesia* multiplies in erythrocytes.
During the process, it has to counteract the toxic effects of
reactive oxygen and nitrogen species (ROS, RNS) that could
potentially lead to major oxidative DNA damage and lipid

✉ Jinlin Zhou
jinlinzhou@shvri.ac.cn

1   Key Laboratory of Animal Parasitology of Ministry of Agriculture,
Shanghai Veterinary Research Institute, Chinese Academy of
Agricultural Sciences, Shanghai 200241, China

2   Jiangsu Co-innovation Center for Prevention and Control of
Important Animal Infectious Diseases and Zoonoses,
Yangzhou 225009, China

peroxidation (Gray et al. 2010; Regner et al. 2014). Thus, in order to counteract the oxidative stress and maintain a redox balance, parasites employ a thioredoxin (Trx) system, which includes the nicotinamide-adenine dinucleotide phosphate (NADPH), the Trx redox protein, and the NADPH-dependent disulfide oxidoreductase, namely Trx reductase (TrxR) (Fritz-Wolf et al. 2013). TrxR belongs to the dimeric flavoenzymes family and catalyzes the transfer of electrons from NADPH via FAD to the disulfide substrate. In protozoans, the C-terminal redox center is formed by two cysteines separated by four amino acids and this feature distinguishes it from human TrxR, which contain a cysteine-selenocysteine motif. The Trx system has been extensively studied in *Plasmodium falciparum*, while the enzyme system has not been studied in *Babesia microti* that causes babesiosis (Jortzik et al. 2010; Nickel et al. 2006; Peng et al. 2015).

The partial messenger RNA (mRNA) of TrxR gene is present in the genome of *B. microti* (NCBI Reference Sequence: XM_012793011.1). Then, we obtained the full-length gene BmiTrxR by amplifing the 5′ and 3′ regions of mRNA by RACE. Here, we report the protein on recombinant expression, purification, and biochemical characterization of its function in the redox metabolism of the parasite.

Materials and methods

Parasites and animals

The *B. microti* strain was obtained from the American Type Culture Collection (ATCC^R PRA-99™) and was injected into Kunming mice. The parasites were isolated when 20–30 % of RBCs were infected, as determined by Giemsa-stained thin-blood films.

Bacteria and plasmids

Escherichia coli top 10 cells (Invitrogen) and *E. coli* BL21 (DE3) (Novagen) were used in routine plasmid construction and expression experiments, respectively. The vector pMD-18T (TaKaRa, Dalian, China) was used for cloning and sequencing purposes. The expression vector used was pET28a vector (Novagen).

Molecular cloning of TrxR from *B. microti*

RNA extraction from *B. microti* merozoites was performed using TRIzol reagent (Invitrogen). Complementary DNAs (cDNAs) were obtained by RT-PCR using RNA extracted from *B. microti* merozoites. The reactions were performed according to the instructions in the Reverse Transcription System Kit (TaKaRa, Dalian, China). The open reading frame (ORF) sequence of TrxR gene is present in the genome of

B. microti (NCBI Reference Sequence: XM_012793011.1), but there is no complete sequence of BmiTrxR cDNA. Therefore, at first, we designed oligonucleotide primers from reported sequence to amplify the ORF of BmiTrxR (Cornillot et al. 2012). Their sequences are F: 5′-ATGATT CTTCGGGCTGGATT-3′ and R: 5′-TCAACCACA CTTGCCCCCAC-3′.

The 5′ and 3′ regions of mRNA were amplified using a SMARTer RACE cDNA amplification kit (Clintech, San Jose, CA, USA) following the manufacturer's instructions. The primers were designed based on the ORF sequence obtained from above. The primer sequences are GSP1: 5′-GTTTCTTAGGTACACAACCCACG-3′, GSP2: 5′-GCCTCCTCCAATCACAGCGAAGT-3′, and GSP3: 5′-GCTTAGTTTCGGTGAGTGATGCG-3′ for 5′ rapid amplification of cDNA ends (RACE); GSP1: 5′-TAGCA CATAGGATGAAGACAAGGCA-3′ and GSP2: 5′-CAGGGAATGGCATTAGCTATGAAAC-3′ for 3′ RACE. Amplified PCR products were subsequently purified and ligated into the pMD-18T vector (TaKaRa, Dalian, China) and sequenced.

Expression and purification

Full-length BmiTrxR was excised from pMD-18T vector by digestion with Nco I and Xho I and subcloned into pET-28a (Novagen) expression vector. Accuracy of the sequences was confirmed by complete sequencing. The BmiTrxR gene was expressed as a His-tag fusion protein in *E. coli* BL21 (DE3) according to the manufacturer's instructions. The recombinant proteins were induced with 1 mM IPTG, followed by incubation at 16 °C for 12 h. The cells were harvested and stored at −80 °C until further use. Purification of recombinant BmiTrxR was carried out by chromatography onto a Ni-NTA His·Bind Resin (Novagen). Then, the cell pellet was collected, resuspended in binding buffer (NI-NTA Buffer Kit, Novagen), disrupted by sonication and centrifuged at 12,000×g for 10 min at 4 °C. The soluble fraction was loaded onto a chromatographic column that was previously equilibrated with binding buffer. The column was washed two times with wash buffer and the recombinant protein was eluted in elution buffer (NI-NTA Buffer Kit, Novagen). Active fractions were pooled and quantified.

Production of antiserum against recombinant BmiTrxR and western blotting

The purified recombinant BmiTrxR protein was mixed with Freund's complete adjuvant (Sigma) and 200 μg recombinant BmiTrxR was injected intraperitoneally into a mouse. Subsequently, booster injections were administered twice into the mouse at 2-week intervals each containing the same amount of Freund's incomplete adjuvant and antigen. After

the second boost, blood samples were collected via the orbital vein. Antibody titers of sera against recombinant BmiTrxR were measured by ELISA.

The lysates of *B. microti*-infected mouse erythrocytes or un-infected mouse erythrocytes were mixed with an equal volume of $2 \times$ SDS gel-loading buffer. Then, the samples were boiled for 10 min and separated on a 12 % SDS-polyacrylamide gel by electrophoresis. The gel was transferred to a nitrocellulose (NC) membrane, blocked in 5 % milk solution overnight at 4 °C and the NC membrane was incubated with the recombinant BmiTrxR antiserum (1:200 dilution) for 1 h at room temperature, followed by five 10 min washes with PBST. Then, the membrane was incubated with HRP-conjugated goat anti-mouse IgG (1:2000 dilution) at room temperature for 1 h. After washing five times as above, positive signals were detected with the DAB substrate.

IFAT and confocal laser microscopic observation

Recognition of *B. microti* merozoites by anti-rBmiTrxR serum was tested by indirect immunofluorescence by confocal laser micrographs. Thin blood smears were fixed in a mixture of methanol and acetone (*v*:*v*/1:1) at −20 °C for 10 min. After three washes in PBS, blood cells were permeabilized with 0.1 % TritonX-100 for 20 min. Then, the fixed smears were incubated with the anti-rBmiTrxR-specific mouse serum (primary antibody) and incubated for 45 min followed by three 5 min washes in PBS. The slides were then incubated with goat anti-mouse immunoglobulin G conjugated with Alexa 488 (Molecular Probes Inc.) for 45 min and washed in PBS. Subsequently, the slides were incubated with 4′, 6′-diamidino-2-phenylindole (DAPI) (Thermo) for 20 min, washed in PBS and then covered with FluoromountTM Aqueous Mounting Medium (Sigma). Finally, the slides were examined under a confocal laser scanning microscope (Jia et al. 2009).

Recombinant BmiTrxR enzyme assays and inhibition test

The enzyme assays were performed at 25 °C using a Multiskan Spectrum (SpectraMax M5, Molecular Devices). TrxR activity in the recombinant BmiTrxR was determined by the 5, 5′-diothiobis (2-nitrobenzoic acid) (DTNB) reduction assay and the insulin reduction assay. Briefly, the DTNB reduction assay solution (200 μl) contained 100 mM potassium phosphate (pH 6.5), 2 mM DTNB and 2 mM EDTA. The reaction was initiated by the addition of BmiTrxR and the activity was monitored by the increase in absorbance at 412 nm during the first 3 min. Activity was calculated using the extinction coefficient of 13.6 mM^{-1} cm^{-1} for thionitrobenzoate (TNB), considering that 1 mol of NADPH yields 2 mol of TNB.

Trx reduction assay was carried out in the presence of 0.16 mM bovine insulin (Sigma), 10 μM recombinant BmiTrx, and 100 μM NADPH in 50 mM Tris-HCl (pH 6.5)

containing 2 mM EDTA. Trx activity was determined by the decrease in the absorbance at 340 nm that was due to the consumption of NADPH. The extinction coefficient of 6.22 mM^{-1} cm^{-1} for NADPH was used in the calculations. For all enzyme assays, the controls did not have BmiTrxR or substrate in the reactions. The assays were repeated at least three times for each enzyme. In these TrxR activity assays, NADPH concentration ranged from 5 to 100 μM, DTNB concentrations ranged from 100 to 1000 μM, and Trx from 5 to 30 μM. The concentration of BmiTrxR was maintained at a constant 50 nM. In each reaction, the concentration of only one substrate was changed while keeping the others constant. All the kinetic parameters were acquired by fitting the experimental data with a nonlinear least-squares formula and Michaelis-Menten equation. Kinetic constants are represented as the mean of at least three independent data sets (Lothrop et al. 2014; Regner et al. 2014; Snider et al. 2014; Song et al. 2012).

Auranofin, a TrxR inhibitor, was used to monitor the reduction of DTNB at 412 nm. The assay medium contained 100 μM NADPH, 2 mM DTNB, and 50 nM BmiTrxR, in which the inhibitor concentrations were 0, 1.563, 3.125, 6.25, and 12.5 μM. The recombinant enzyme was preincubated with the inhibitor in the assay buffer for 15 min. Then, NADPH and DTNB were added to each well and residual enzyme activity was monitored (Song et al. 2012).

Results
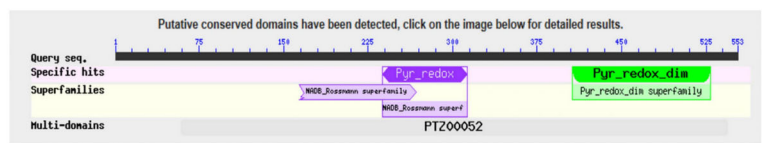
Cloning and characterization of the BmiTrxR gene

Using the partial mRNA of TrxR gene present in the genome of *B. microti* (NCBI Reference Sequence: XM_012793011.1), we identified the ORF of BmiTrxR, which contains 5 introns, a single open reading frame with 1659 bp that encoded a polypeptide with 553 amino acids. The putative protein has a molecular mass of 58.4 kDa and an isoelectric point of 6.95, which is similar to other H-TrxRs members. The predicted signal peptide cleavage site was between 18 and 19 amino acids. Then, the cDNA was obtained by RT-PCR using the mRNA of *B. microti* merozoites. In order to obtain the complete cDNA of BmiTrxR, we amplified the 5′ and 3′ regions of mRNA by RACE and the full-length BmiTrxR cDNA was 1766 bp (GenBank accession KU845266). BLAST analysis of the predicted protein against all NCBI non-redundant databases revealed significant similarity scores with members of TrxR from other species. The amino acid sequence of BmiTrxR was 58 % identical to *Babesia bovis* TrxR (XP_001608869.1), 53 % identical to *P. falciparum* TrxR (XP_002808951.1), 54 % to *Cryptosporidium hominis* TrxR (XP_666572.1), 55 % to

Fig. 1 The structure and amino acid sequence alignment of a novel BmiTrxR with TrxR homologues. **a** cDNA and putative amino acid sequences. **b** The predicted active domain by NCBI protein blast. **c** Putative amino acid alignment of BmiTrxR with other TrxR: *B. bovis* TrxR (XP_001608869.1); *P. falciparum* TrxR (XP_002808951.1); *C. hominis* TrxR (XP_666572.1); *T. annulata* strain Ankara (XP_954814.1). The conserved active sites are *boxed* (N-terminal: -CVNVGC-; C-terminal: -GC×GG×CG)
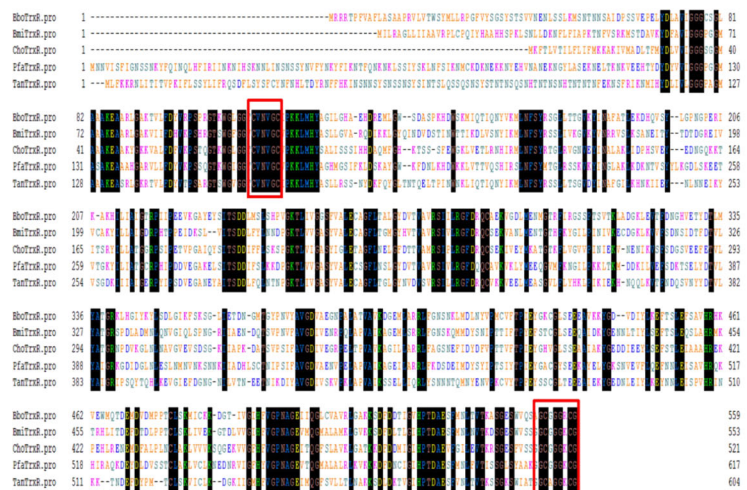

(A)

(B)

(C)

Theileria annulata strain Ankara (XP_954814.1), and 44 % to Human TrxR (3QFB_B) (Fig. 1). We found that the putative protein had a thiol-disulfide redox active center (-CVNVGC-) in its N-terminus and the C-terminus contained a conserved GCGGGKCG sequence, which is the catalytic domain of TrxR. A more detailed investigation of phylogram of the TrxR suggested a complex history for this gene family and an ancient origin and high degree of conservation during evolution. The phylogenetic analysis shows the close relativity between *B. microti* TrxR and *T. annulata* TrxR, which is based on their sequences high similarity (Fig. 2).

Identification of the native BmiTrxR in *B. microti*

The recombinant protein was successfully expressed and had a molecular weight of 58.4 kDa, which is in agreement with the expected size predicted from the amino acid sequence (Fig. 3). A mouse anti-BmiTrxR polyclonal serum was obtained after immunizing mice with the purified recombinant BmiTrxR. This antiserum was used to identify the native BmiTrxR in the lysate of *B. microti*. As shown in Fig. 4, a specific protein band with a molecular weight of ~58.4 kDa was detected in *B. microti*-infected red blood cells but not in the un-infected cells by western blotting. The size of the
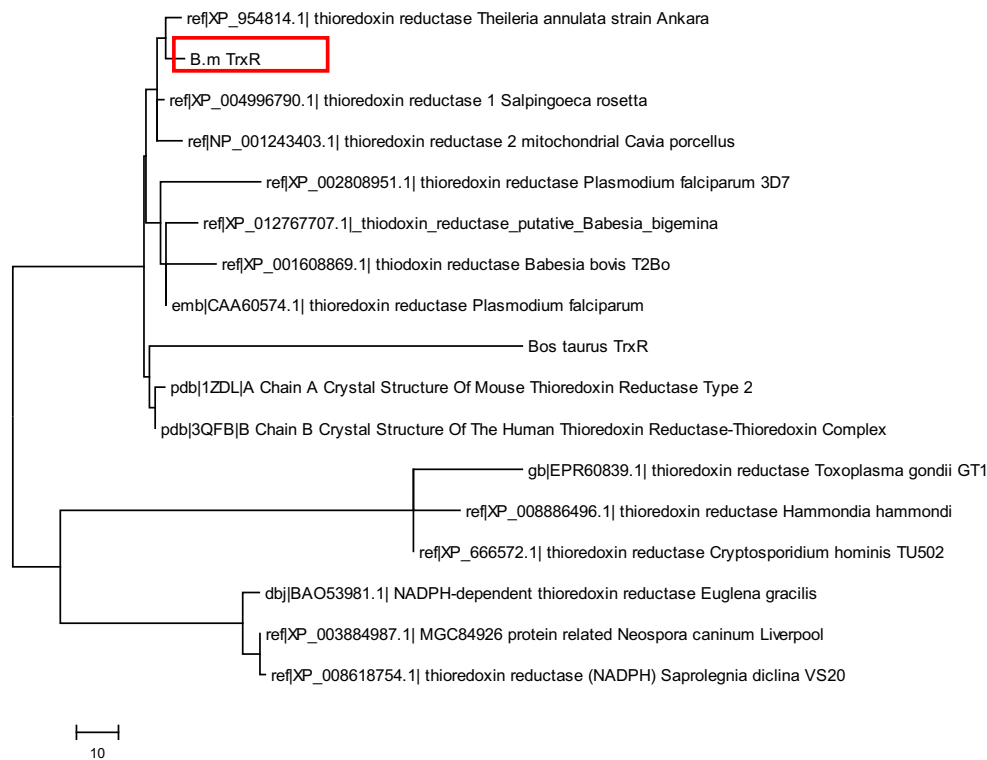
Fig. 2 Relationship of BmiTrxR to other species TrxR homologues. The rectangular phylogram is based on the alignment of sequences derived from this study using MEGA by maximum likelihood and similar sequences obtained from the NCBI database

recombinant BmiTrxR band was similar to that of the natural BmiTrxR. There were no other protein bands recognized by the antiserum. These results suggested that the recombinant BmiTrxR was immunoreactive, inducing antibodies specific to the native BmiTrxR protein. In order to determine the cellular localization of BmiTrxR, a thin blood smear was used to perform IFAT with the mouse anti-rBmiTrxR serum and observed under a confocal laser microscope. The specific fluorescence seemed to localize in the cytoplasm of *B. microti* merozoites (Fig. 5).
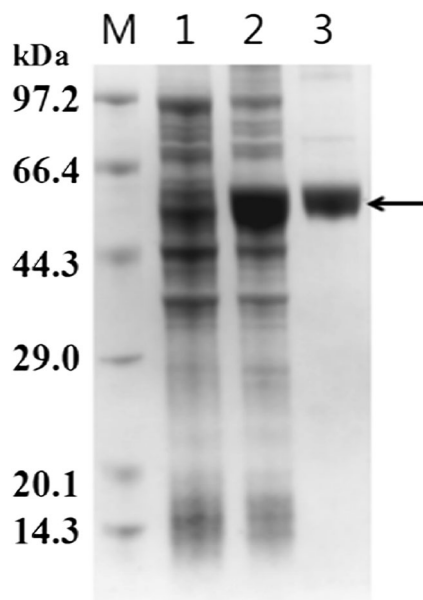

Fig. 3 Expression and purification of the recombinant protein of BmiTrxR, a novel gene isolated from the *Babesia microti*, in a His-fused soluble form, in *E. coli*. The bacterial lysate or recombinant protein was electrophoresed in a 12 % SDS-PAGE and stained with Coomassie blue. *Lane 1*: the uninduced cell lysate; *lane 2*: the induced cell lysate; *lane 3*: purified recombinant protein BmiTrxR. *M*: protein molecular weight marker
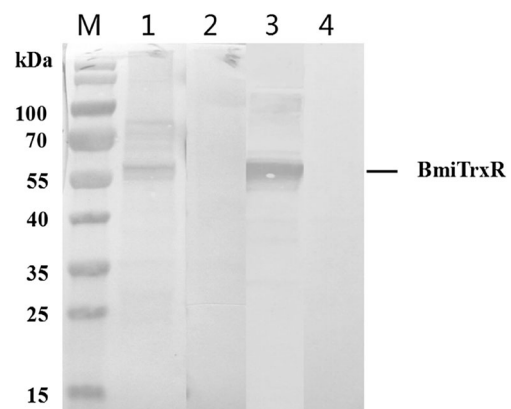

Fig. 4 Western blot analysis of BmiTrxR. *Lane 1* and *lane 4*: *Babesia microti*-infected mouse erythrocyte lysate; *lane 2*: normal mouse erythrocyte lysate: *lane 3*: purified recombinant BmiTrxR protein. *Lane 1*, *2*, and *3* were western blot analysis probed with an anti-rBmiTrxR mouse serum; *lane 4* was incubated with His-tag monoclonal antibody. *M*: protein molecular weight marker
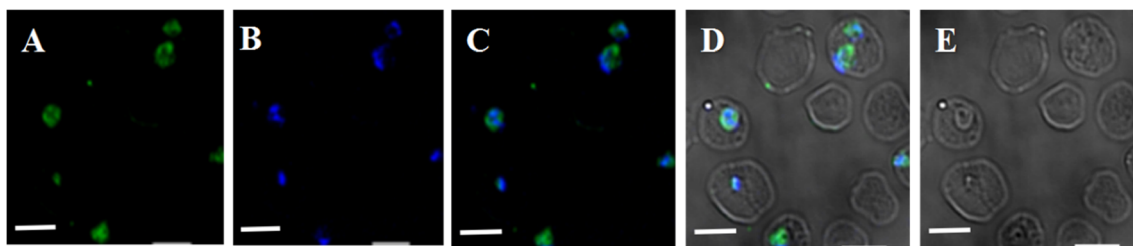
Fig. 5 Observation of the native BmiTrxR recognized by a mouse anti-rBmiTrxR serum in confocal laser micrographs. **a** Immunofluorescent staining of *B. microti* merozoites with mouse anti-rBmiTrxR serum. **b** 4′, 6′-diamidino-2-phenylindole (DAPI) staining of *B. microti* merozoite nuclei. **c** Panel **a** overlaid on panel **b**. **d** Panels **a** and **b** overlaid on phase-contrast images of *B. microti* merozoites. **e** Phase-contrast images of *B. microti* merozoites. The images were derived from a single section. Bars, 4.6 μm

Activity and kinetics of recombinant BmiTrxR

Enzyme activity of the purified recombinant BmiTrxR was maximum at pH 6.5 in 100 mM phosphate buffer and 25 °C (Fig. 6). Moreover, the highest initial velocity of the enzyme was at the concentration of 100 nM (Fig. 7). The activity of BmiTrxR against NADPH-dependent disulfide reductase using DTNB as substrate was significantly higher than the TrxR of Rat (RatTrxR) at the same concentration (Fig. 8). BmiTrxR was also able to reduce both BmiTrx and the ortholog protein from *E. coli* (EcoTrx) (Fig. 9).

Inhibition assay of chemical compounds on BmiTrxR disulfide reductase activity

In addition, we investigated the efficiency of the auranofin inhibitor, which has been reported to inhibit *P. falciparum* TrxR. The experimental data showed that auranofin abrogated the enzyme activity of BmiTrxR completely at 12.5 μM (Fig. 10), suggesting that auranofin could be evaluated as a potential inhibitor of the BmiTrxR disulfide reductase activity.
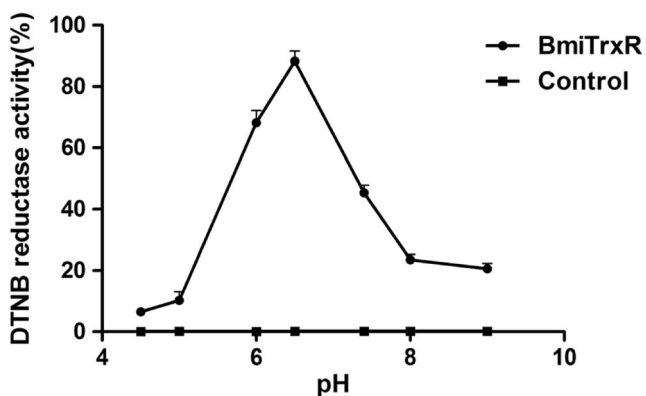
Discussion

Infectious parasites are reported to be exposed to reactive oxygen and nitrogen species (ROS, RNS) created by the host immune response against the infection (Becker et al. 2004; Jortzik and Becker 2012). During the erythrocytic stages of apicomplexan protozoans, the thioredoxin (Trx)-thioredoxin reductase (TrxR) system plays a central role in the oxidative stress response (Regner et al. 2014). The NADPH-dependent disulfide reductase is the principal electron donor for the thioredoxin redox networks comprising, among others, thioredoxin, ribonucleotide reductase, and peroxiredoxins (Muller 2004). Previous work in the *P. falciparum* system had suggested that *PfTrxR* is vital for parasite growth under in vitro culture conditions (Krnajski et al. 2002) and the antioxidant defense in *B. bovis* is also supported by the *BboTrxR* (Regner et al., 2014). In this study, we describe the identification and biochemical properties of TrxR, which is likely involved in the Trx system of *B. microti*. To the best of our knowledge, this is the first identification and characterization of BmiTrxR activity and functionality in *B. microti*.

BLAST comparisons indicated the presence of only one TrxR gene in the *B. microti* genome. This gene belonged to the H-TrxR group with a redox-active center, which has a characteristic motif (CXXXXC) in the FAD-binding domain and a C-terminal domain (the interface domain) (Fig. 1).

Fig. 6 pH-dependent activity profile of BmiTrxR for DTNB reductase activity. Assays were performed at 25 °C 100 mM potassium phosphate at different pH values with 0.1 mM NADPH, 2 mM DTNB, and 50 nM BmiTrxR, while the contral assay used His polypeptide instead of the enzyme TrxR with the same concentration. The calculated optimal pH value was 6.5. The calculated value is the mean of at least three independent sets of data
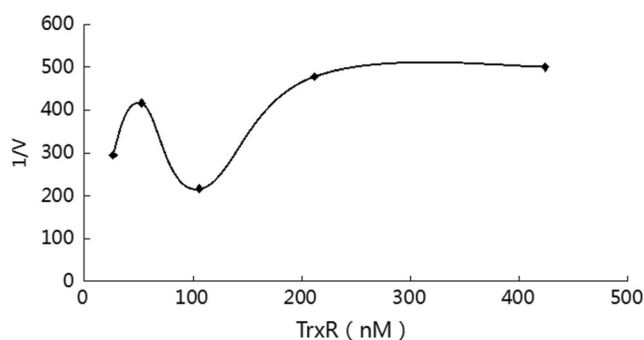

Fig. 7 The relationship of concentration and initial velocity of the enzyme BmiTrxR for DTNB reductase activity. The reaction contained 100 mM potassium phosphate with, 0.1 mM NADPH, 2 mM DTNB at pH 6.5 and 25 °C
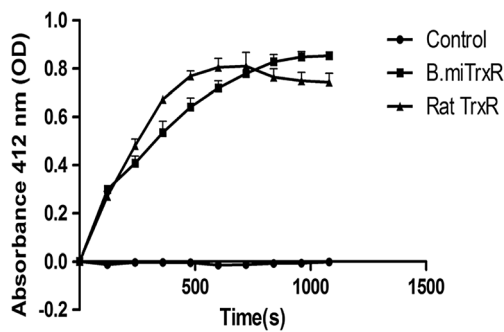
Fig. 8 DTNB reductase activity of BmiTrxR and TrxR of Rat (RatTrxR). The reaction was monitored with the reduction of DTNB (at 412 nm) with 2 mM DTNB, 100 nM BmiTrxR, 0.1 mM NADPH at pH 6.5 and 25 °C. The contral assay used His polypeptide instead of the enzyme TrxR with the same concentration

Fig. 10 Auranofin as inhibitor of disulfide reductase activity of BmiTrxR. The assay medium contained 100 μM NADPH, 2 mM DTNB, 50 nM *BmTrxR*, in which the inhibitor concentrations respectively were 0, 1.563, 3.125, 6.25, and 12.5 μM

BmiTrxR shares more than 50 % sequence identity with homologous sequences from other protozoans, while with the host human TrxR the similarity was only 44 %. This is likely due to the presence of a characteristic cysteine-selenocysteine (Cys-SeCys) domain in the C-terminus of human TrxR. Because of the absence of a selenocysteine residue in the parasite's TrxR site, the human and parasite enzymes have distinct substrate specificities, which validates the protein as an excellent drug target (Buchholz et al. 2010; Hirt et al. 2002; Jortzik and Becker 2012; Nepveu and Turrini 2013). In addition, Fig. 2 might provide a clearer picture of the evolution of this key detoxification TrxR. Phylogenetic analysis indicates that TrxR exists a broader range of species including apicomplexan parasites and their mammal hosts. Unexpectedly, the result shows a close homologous relationship between *B. microti* TrxR and *T. annulata* TrxR, indicating these enzymes may share common ancestry and function. Because the two parasites all belong to piroplasms multiplying in the host's erythrocyte, transmitted by tick and similar life history (Li et al. 2014; Zanet et al. 2014). Western blotting result showed that the antiserum could recognize the native BmiTrxR in *B. microti*. Moreover, the previous study reported
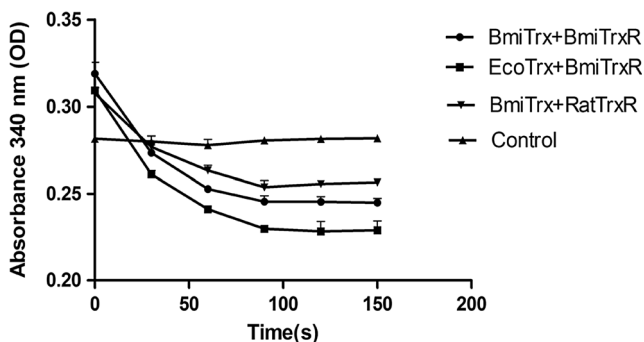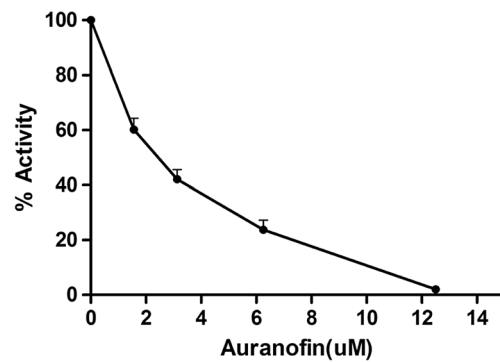

Fig. 9 Trx reduction assay. Assays were performed at 25 °C in 0.16 mM bovine insulin, 10 μM recombinant *BmiTrx* or *EcoTrx*, 100 nM BmiTrxR or RatTrxR, 100 uM NADPH in the 50 mM Tris-HCI (pH 6.5) containing 2 mM EDTA, while the contral assay used His polypeptide instead of the enzyme TrxR with the same concentration

that *P. falciparum* TrxR were located in the cytosol and in mitochondria (Kehr et al. 2010); thus, this could also be the case for the occurrence of TrxR in *B. microti*.

Using the same methods previously published for production of recombinant SmTGR and conditions for enzyme kinetics analysis (Regner et al. 2014), the experimental data in the present study showed that the recombinant BmiTrxR was active as NADPH-dependent disulfide reductase, using DTNB as substrate (Fig. 8) and it was also able to reduce both BmiTrx and the ortholog protein from *E. coli* (EcoTrx) (Fig. 9). However, it is worth to point that we constructed the recombinant BmiTrxR-pET28a plasmid to express TrxR fused to N-term and C-term His-tags to reach high purification degree. On the one hand, we easily detected the enzyme activity with substrate DTNB. Unexpectedly, the recombinant protein exhibited no activity with EcoTrx, even when different experimental conditions were tested, which leads us to revisit the protein primary. By the analysis of three-dimensional structure of BmiTrxR in complex with its physiologic substrate BmiTrx (unpublished), we found the binding site in the C-term of the recombinant enzyme was affected by the C-term His-tag. After removing the C-term His-tag and remaining the N-term His-tag, the enzyme finally showed disulfide reductase activity with EcoTrx.

This reductase activity exhibited a maximum at pH 6.5 in 100 mM phosphate buffer and 25 °C, which is different with the pH 8.0 reported in previous study (Regner et al. 2014). In DTNB reductase activity assay, the initial velocity of reaction of Rat TrxR is higher than BmiTrxR (Fig. 8), which supported that the selenocysteine-cysteine (SeCys-Cys) motif of mammalian TrxR is highly reactive when compared to the Cys-xxxx-Cys motif in BmiTrxR. In addition, Table 1 show that the K_{cat}/K_m with NADPH (2.2×10^5 M^{-1}·s^{-1}) was about five times than that with DTNB (4.04×10^4 M^{-1}·s^{-1}). V_{max} and K_{cat} with NADPH were 20.08 ± 3.27 μM·min^{-1}, 6.69 s^{-1}, respectively, which was approximately three times than that with EcoTrx (6.37 ± 0.80 μM·min^{-1}, 2.12 s^{-1}). These values

Table 1 Kinetic parameters of recombinant BmiTrxR with different substrates

Substrate	K_m μM	V_{max} μM·min^{-1}	K_{cat} s^{-1}	K_{cat}/K_m M^{-1}·s^{-1}
NADPH	30.36 ± 7.40	20.08 ± 3.27	6.69	2.2×10^5
DTNB	135.15 ± 9.27	16.39 ± 0.12	5.46	4.04×10^4
EcoTrx	10.53 ± 3.33	6.37 ± 0.80	2.12	2.01×10^5

Kinetic constants for recombinant BmiTrxR (50 nM) were determined in assays performed at 25 °C in 50 mM Tris-HCl (pH 6.5) with 2 mM EDTA and 100 μM NADPH. All assays were conducted in triplicate

are practically in the same order of magnitude and similar to those determined for H-TrxRs from other species (Regner et al. 2014). The findings may suggest that NADPH, combined with BmiTrxR via FAD domain, tends to deliver electrons to the disulfide substrate DTNB and Trx. In *P. falciparum*, the electrons are shuttled from NADPH via FAD to the N-terminal active site. Subsequently, the electrons are transferred to the C-terminal redox motif that finally reduces the substrate Trx (Gilberger et al. 1997). Further study on the direction of electron transfer of BmiTrxR will be surveyed.

Interfering with redox metabolism represents a promising approach to antiparasitic drug development (Krauth-Siegel et al. 2005) prominent examples being *P. falciparum* thioredoxin reductase (Buchholz et al. 2010) and *Schistosoma mansoni* thioredoxin-glutathione reductase (Kuntz et al. 2007). Also *Babesia* TrxR was considered a leading drug target because (i) complete structural information, which permits computational inhibitor modeling (Sarma et al. 2003), (ii) some drugs have been proved to inhibit the TrxR of apicomplexan protozoa and mammal (Andricopulo et al. 2006), (iii) structural differences between the selenoprotein H-TrxR and *Babesia* TrxR occurring at the solvent exposed C-terminal end of the proteins were considered most attractive sites for directed inhibitor development (McMillan et al. 2006; Rahlfs and Becker 2006). Auranofin, a gold-based compound, was found to inhibit *P. falciparum* growth in vitro (Sannella et al. 2008). Auranofin-mediated inhibition of TrxR activity was competitive, which has a benzene ring structure (Angelucci et al. 2009) and is similar to DTNB with two benzene rings connected by a disulfide bond (Spiga et al. 2011). Our data also suggest that auranofin can inhibit the disulfide reductase activity of recombinant BmiTrxR in a low inhibition concentration (Fig. 10), which is similar to the findings in *E. granulosus* (Agorio et al. 2003) and *S. mansoni* (Angelucci et al., 2009). As mentioned above, auranofin could be a potential inhibitor of the native protein BmiTrxR in the parasite, which may be used as an anti-*B. microti* drug.

To our knowledge, this is the first report on the analysis, identification, molecular cloning, and functional characterization of the TrxR from *B. microti*. Sequences alignment and phylogenetic analysis shows that BmiTrxR shares 55 %

sequence identity and most closely relationship with homologous sequences from *T. annulata*, suggesting these proteins may possess common ancestry and function. The recombinant enzyme exhibited NADPH-dependent disulfide reductase activity with the model DTNB and classic Trx, indicating that the enzyme may play a certain role in maintaining the redox balance in *B. microti*. These findings improve the knowledge of TrxR in *B. microti* and provide some useful reference for the further research.

References

Agorio A, Chalar C, Cardozo S, Salinas G (2003) Alternative mRNAs arising from trans-splicing code for mitochondrial and cytosolic variants of *Echinococcus granulosus* thioredoxin Glutathione reductase. J Biol Chem 278(15):12920–8

Andricopulo AD, Akoachere MB, Krogh R, Nickel C, McLeish MJ, Kenyon GL, Arscott LD, Williams CH Jr, Davioud-Charvet E, Becker K (2006) Specific inhibitors of *Plasmodium falciparum* thioredoxin reductase as potential antimalarial agents. Bioorg Med Chem Lett 16(8):2283–92

Angelucci F, Sayed AA, Williams DL, Boumis G, Brunori M, Dimastrogiovanni D, Miele AE, Pauly F, Bellelli A (2009) Inhibition of *Schistosoma mansoni* thioredoxin-glutathione reductase by auranofin: structural and kinetic aspects. J Biol Chem 284(42):28977–85

Becker K, Tilley L, Vennerstrom JL, Roberts D, Rogerson S, Ginsburg H (2004) Oxidative stress in malaria parasite-infected erythrocytes: host-parasite interactions. Int J Parasitol 34(2):163–89

Buchholz K, Putrianti ED, Rahlfs S, Schirmer RH, Becker K, Matuschewski K (2010) Molecular genetics evidence for the in vivo roles of the two major NADPH-dependent disulfide reductases in the malaria parasite. J Biol Chem 285(48):37388–95

Cornillot E, Hadj-Kaddour K, Dassouli A, Noel B, Ranwez V, Vacherie B, Augagneur Y, Bres V, Duclos A, Randazzo S, Carcy B, Debierre-Grockiego F, Delbecq S, Moubri-Menage K, Shams-Eldin H, Usmani-Brown S, Bringaud F, Wincker P, Vivares CP, Schwarz RT, Schetters TP, Krause PJ, Gorenflot A, Berry V, Barbe V, Ben Mamoun C (2012) Sequencing of the smallest *Apicomplexan*

genome from the human pathogen *Babesia microti*. Nucleic Acids Res 40(18):9102–14

Fritz-Wolf K, Jortzik E, Stumpf M, Preuss J, Iozef R, Rahlfs S, Becker K (2013) Crystal structure of the *Plasmodium falciparum* thioredoxin reductase-thioredoxin complex. J Mol Biol 425(18):3446–60

Gilberger TW, Walter RD, Muller S (1997) Identification and characterization of the functional amino acids at the active site of the large thioredoxin reductase from *Plasmodium falciparum*. J Biol Chem 272(47):29584–9

Gray J, Zintl A, Hildebrandt A, Hunfeld KP, Weiss L (2010) Zoonotic babesiosis: overview of the disease and novel aspects of pathogen identity. Ticks Tick Borne Dis 1(1):3–10

Hirt RP, Muller S, Embley TM, Coombs GH (2002) The diversity and evolution of thioredoxin reductase: new perspectives. Trends Parasitol 18(7):302–8

Holmgren A, Lu J (2010) Thioredoxin and thioredoxin reductase: current research with special reference to human disease. Biochem Biophys Res Commun 396(1):120–4

Homer MJ, Aguilar-Delfin I, Telford SR 3rd, Krause PJ, Persing DH (2000) Babesiosis. Clin Microbiol Rev 13(3):451–69

Jia H, Terkawi MA, Aboge GO, Goo YK, Ma L, Zhou J, Nishikawa Y, Igarashi I, Fujisaki K, Xuan X (2009) Identification of secreted antigen 3 from *Babesia gibsoni*. Clin Vaccine Immunol 16(6):944–8

Jortzik E, Becker K (2012) Thioredoxin and glutathione systems in Plasmodium falciparum. Int J Med Microbiol 302(4-5):187–94

Jortzik E, Fritz-Wolf K, Sturm N, Hipp M, Rahlfs S, Becker K (2010) Redox regulation of *Plasmodium falciparum* ornithine delta-aminotransferase. J Mol Biol 402(2):445–59

Kehr S, Sturm N, Rahlfs S, Przyborski JM, Becker K (2010) Compartmentation of redox metabolism in malaria parasites. PLoS Pathog 6(12):e1001242

Krauth-Siegel RL, Bauer H, Schirmer RH (2005) Dithiol proteins as guardians of the intracellular redox milieu in parasites: old and new drug targets in trypanosomes and malaria-causing plasmodia. Angew Chem Int Ed Engl 44(5):690–715

Krnajski Z, Gilberger TW, Walter RD, Cowman AF, Muller S (2002) Thioredoxin reductase is essential for the survival of *Plasmodium falciparum* erythrocytic stages. J Biol Chem 277(29):25970–5

Kuntz AN, Davioud-Charvet E, Sayed AA, Califf LL, Dessolin J, Arner ES, Williams DL (2007) Thioredoxin glutathione reductase from *Schistosoma mansoni*: an essential parasite enzyme and a key drug target. PLoS Med 4(6):e206

Li Y, Chen Z, Liu Z, Liu J, Yang J, Li Q, Li Y, Ren Q, Niu Q, Guan G, Luo J, Yin H (2014) First report of *Theileria* and *Anaplasma* in the Mongolian gazelle, *Procapra gutturosa*. Parasit Vectors 7:614

Lothrop AP, Snider GW, Ruggles EL, Hondal RJ (2014) Why is mammalian thioredoxin reductase 1 so dependent upon the use of selenium? Biochemistry 53(3):554–65

McMillan PJ, Arscott LD, Ballou DP, Becker K, Williams CH Jr, Muller S (2006) Identification of acid-base catalytic residues of high-Mr thioredoxin reductase from *Plasmodium falciparum*. J Biol Chem 281(44):32967–77

Muller S (2004) Redox and antioxidant systems of the malaria parasite *Plasmodium falciparum*. Mol Microbiol 53(5):1291–305

Nepveu F, Turrini F (2013) Targeting the redox metabolism of *Plasmodium falciparum*. Future Med Chem 5(16):1993–2006

Nickel C, Rahlfs S, Deponte M, Koncarevic S, Becker K (2006) Thioredoxin networks in the malarial parasite *Plasmodium falciparum*. Antioxid Redox Signal 8(7-8):1227–39

Peng M, Cascio D, Egea PF (2015) Crystal structure and solution characterization of the thioredoxin-2 from *Plasmodium falciparum*, a constituent of an essential parasitic protein export complex. Biochem Biophys Res Commun 456(1):403–9

Rahlfs S, Becker K (2006) Interference with redox-active enzymes as a basis for the design of antimalarial drugs. Mini Rev Med Chem 6(2):163–76

Regner EL, Thompson CS, Iglesias AA, Guerrero SA, Arias DG (2014) Biochemical characterization of thioredoxin reductase from Babesia bovis. Biochimie 99:44–53

Sannella AR, Casini A, Gabbiani C, Messori L, Bilia AR, Vincieri FF, Majori G, Severini C (2008) New uses for old drugs. Auranofin, a clinically established antiarthritic metallodrug, exhibits potent antimalarial effects in vitro: mechanistic and pharmacological implications. FEBS Lett 582(6):844–7

Sarma GN, Savvides SN, Becker K, Schirmer M, Schirmer RH, Karplus PA (2003) Glutathione reductase of the malarial parasite *Plasmodium falciparum*: crystal structure and inhibitor development. J Mol Biol 328(4):893–907

Schnittger L, Rodriguez AE, Florin-Christensen M, Morrison DA (2012) *Babesia*: a world emerging. Infect Genet Evol 12(8):1788–809

Snider GW, Dustin CM, Ruggles EL, Hondal RJ (2014) A mechanistic investigation of the C-terminal redox motif of thioredoxin reductase from *Plasmodium falciparum*. Biochemistry 53(3):601–9

Song L, Li J, Xie S, Qian C, Wang J, Zhang W, Yin X, Hua Z, Yu C (2012) Thioredoxin glutathione reductase as a novel drug target: evidence from *Schistosoma japonicum*. PLoS One 7(2):e31456

Spiga O, Summa D, Cirri S, Bernini A, Venditti V, De Chiara M, Priora R, Frosali S, Margaritis A, Di Giuseppe D, Di Simplicio P, Niccolai N (2011) A structurally driven analysis of thiol reactivity in mammalian albumins. Biopolymers 95(4):278–85

Zanet S, Trisciuoglio A, Bottero E, de Mera IG, Gortazar C, Carpignano MG, Ferroglio E (2014) Piroplasmosis in wildlife: *Babesia* and *Theileria* affecting free-ranging ungulates and carnivores in the Italian Alps. Parasit Vectors 7:70